ELSEVIER

European Journal of Pharmacology 384 (1999) 203–212

ejp

www.elsevier.nl/locate/ejphar

Electrophysiological actions of a novel K^+ channel opener MCC-134 on rabbit portal vein smooth muscle

Hiromitsu Morita [a], Kazunori Yamada [a], Kihachiro Abe [b], Yushi Ito [a], Ryuji Inoue [a,*]

[a] *Department of Pharmacology, Graduate School of Medical Sciences, Kyushu University, Fukuoka 812-8582, Japan*
[b] *Special Patient Oral Care Unit, Kyushu University Dental Hospital, Fukuoka 812-8582, Japan*

Received 23 August 1999; received in revised form 13 September 1999; accepted 16 September 1999

Abstract

The effects of a newly synthesized K^+ channel opener, 1-[4-(1*H*-imidazol-1-yl)benzoyl]-*N*-methylcyclobutane-carbothioamide (MCC-134) on membrane currents and intracellular Ca^{2+} mobilization were investigated in rabbit portal vein smooth muscle cells. Under voltage-clamped conditions, MCC-134 dose-dependently induced K^+-selective currents (I_{MCC}; EC_{50} 5.3 μM) showing little desensitization but fast deactivating properties on washout of drugs. I_{MCC} was completely blocked by 10 μM glibenclamide, not affected by iberiotoxin (500 nM), charybdotoxin (200 nM) or apamin (500 nM), and inhibited by nonspecific K^+ channel blockers, tetraethylammonium (1–10 mM), 4-aminopyridine (0.1–1 mM) and Ba^{2+} (0.01–0.1 mM). Intracellularly applied nucleotide diphosphates (1 mM) were effective at maintaining I_{MCC} (apparent potency; ADP ≦ GDP≒IDP < UDP), whereas intracellular ATP exhibited a biphasic, i.e., augmentative and inhibitory effect(s) on I_{MCC}. Single channel activities of about 15 pS (40/140 mM extra-/intracellular K^+) fully accountable for macroscopic I_{MCC} were activated by MCC-134. MCC-134, at a concentration as high as 100 μM, suppressed voltage-dependent Ca^{2+} and noradrenaline-induced cation currents, and concomitant elevations in the intracellular Ca^{2+} concentration ($[Ca^{2+}]_i$).

Keywords: K^+ channel opener; Patch clamp; K^+ channel; ATP-sensitive; Ca^{2+} mobilization

1. Introduction

Since the first discovery of nicorandil and subsequent clear recognition of cromakalim's action to relax vascular muscle with associated membrane hyperpolarization or K^+ channel activating actions, numerous structurally different K^+ channel openers, including benzopyran, pyridine, pyrimidine and benzothiadiazine derivatives, have been synthesized, in the hope of ameliorating disorders, such as hypertension, urinary incontinence and bronchial asthma, which are clinically less manageable with standard therapeutic protocols (Edwards and Weston, 1993; Evans et al., 1996). This is because K^+ channel openers target specific classes of K^+ channels that participate directly in the control of cell excitability in a broad range of tissues. For example, in many types of smooth muscle, application of K^+ channel openers results in membrane hyperpolarization due to activation of time-independent glibenclamide-sensitive K currents which show little dependence on the membrane potential or $[Ca^{2+}]_i$ (Edwards and Weston, 1993; Aaronson and Benham, 1996; Quayle et al., 1997). These features allow these channels to serve as an important background K conductance, and in turn determine the rate and shape of action potentials and so the rate of Ca^{2+} entry via the voltage-dependent Ca^{2+} channels (Nelson and Quayle, 1995; Nelson et al., 1990).

1-[4-(1*H*-imidazol-1-yl)benzoyl]-*N*-methylcyclobutane-carbothioamide (MCC-134) is a newly synthesized K^+ channel opener having a unique structure that has originally developed from a potent thioformamide K^+ channel opener prototype, aprikalim, with several essential structural modifications (Fig. 1; Shinpuku et al., 1997). The results of in vivo studies using spontaneously hypertensive rats have shown MCC-134 to have a number of antihypertensive properties beneficial for clinical use: a slow onset

* Corresponding author. Tel.: +81-92-642-6076; fax: +81-92-642-6079.
E-mail address: inouery@pharmaco.med.kyushu-u.ac.jp (R. Inoue)

0014-2999/99/$ - see front matter
PII: S0014-2999(99)00671-8

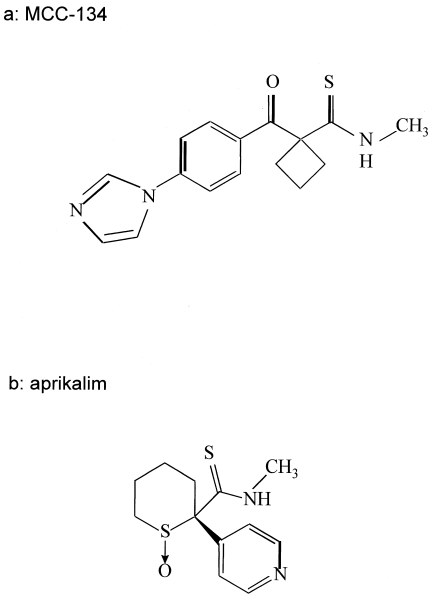

Fig. 1. Chemical structures of MCC-134 (a) and aprikalim (b).

to maximum effect, a long-lasting action and a modest reflex tachycardia (Umeda et al., 1997a). Although in vitro experiments using isolated rat thoracic aortic rings have suggested that these actions may involve not only a K^+ channel opener-like effect but also a direct inhibitory effect on the contractile machinery (Seino et al., 1996), the detailed mechanism of action of the latter remains to be elucidated.

The objective of this study was therefore to investigate the further background behind the relaxant effects of MCC-134 on vascular smooth muscle, in the light of membrane current and $[Ca^{2+}]_i$ measurements. In order to facilitate the comparison between different cells showing variable responses, the response to levcromakalim was taken as a reference, as observed in previous cardiohemodynamic or contractile studies on this compound (Seino et al., 1996; Umeda et al., 1997a). A preliminary account of the present results has been communicated to the 71st annual meeting of the Japanese Pharmacological Society (Morita et al., 1998).

2. Materials and methods

2.1. Materials and cell preparation

Albino rabbits of either sex weighing 1.5–1.8 kg (Nippon White) were anesthetized by intravenous injection of sodium pentobarbital (20–40 mg/kg) and killed by exsanguination. A cylindrical segment of rabbit portal vein (1.5–2 cm in length) was excised after opening the abdominal cavity, and then transferred into a low-Ca^{2+}-containing modified Krebs solution (Ca^{2+}; 0.5–0.75 mM), in which attached connective tissues were removed using fine forceps and scissors. Thin strips measuring ca. 10 mm × 2 mm were prepared and incubated consecutively in Ca^{2+}-free Krebs solution for 10–20 min and this solution supplemented with 2 mg/ml collagenase (Wako, Tokyo, Japan) for 30–40 min at 35°C. After this process was completed, the digested strips were stored in the low Ca^{2+}-containing Krebs solution (see above) at 4°C–10°C in a refrigerator until use. Prior to each experiment, single cells were dispersed using a wide-bore, blunt-tipped Pasteur pipette to draw in and expel the digested strips.

2.2. Electrophysiological recording

The procedures used for electrophysiological recordings were essentially the same as described previously (Inoue and Kuriyama, 1993). Briefly, patch electrodes having a resistance of 5–7 MΩ (filled with K internal solution) were made from boroscilicate glass capillaries, using an automatic multiple-stage electronic puller (P-97, Sutter Instruments, USA) and then heat-polished. A commercial patch clamp amplifier (Axopatch 1D, Axon Instruments, Burlingame, USA) was used in conjunction with an A/D, D/A board (TL-1, Axon Instruments) to generate and apply voltages to and sample current signals from the cell, under the control of an IBM-compatible personal computer using a software pClamp v.5.1. For whole-cell recording, the signals were filtered and digitized at 500 Hz and 1 KHz, respectively and stored on a computer hard disc while, for single channel recording, the signals were stored on a videotape for later analysis after low-pass-filtering at 3 kHz and digitization at 10 kHz through a PCM recorder (VR10, Instrutech, USA). All data were analyzed offline and illustrations were made using pClamp v.6.03 (Axon Instruments), KaleidaGraph v.3.04 (Hulinks). All experiments were performed at room temperature (20°C–25°C).

2.3. Ca^{2+} fluorescence measurement

Ca^{2+} fluorescence measurements were performed by the dual excitation wavelength fluorimetric method. Briefly, fura-2 dissolved in Cs^+-rich internal solution (50 μM) was loaded into the cell via a patch pipette and allowed to equilibrate for 15–20 min. Ca^{2+} fluorescence was measured by a dual spectrofluorometer (CAM 230, Nihon Bunkou, Tokyo) which was attached to an inverted phase-contrast microscope (TMD, Nikon, Tokyo) through an optic fiber cable. Two near-visible UV lights (340 and 380 nm) were shined alternately on fura-2 loaded cells at a frequency of 100 Hz, and the emitted fluorescence was passed through the objective lens (times 40, Fluor 40; Nikon, Japan) and collected by a photomultiplier tube after filtering at 510 nm (±30 nm; CAM 230, Nihon Bunkou, Tokyo). The analog output from the fluorimeter was calibrated, and stored after digitization (500 Hz) on a computer hard disc using the software pClamp v.6.03. Background fluorescence (including the autofluorescence from the cell) was measured for each cell before giga-seal formation, and corrected later. However, this value was less than 2% of the total fluorescence after completion of

fura-2 loading. The value of $[Ca^{2+}]_i$ was estimated according to the method of Grynkiewicz et al. (1985):

$$[Ca^{2+}]_i = K_d B[(R-R_{min})/(R_{max}-R)]$$

where K_d is the dissociation constant of fura-2, B is a constant, R, R_{min} and R_{max} denote the ratio of corrected emission at 340 to 380 nm (F_{340}/F_{380}), and its minimum and maximum values, respectively. The value of R_{max} was determined in each experiment by applying strong hyperpolarizing voltages in the presence of 1.2 mM Ca^{2+} in the bath, which resulted in the development of a large nonspecific inward current and concomitant $[Ca^{2+}]_i$ increase, while R_{min} was estimated as an average of fluorescence after loading 10 mM EGTA into the cell. The quantity $K_d B$ was determined by intracellular calibration (Almers and Neher, 1985) by introducing into the cell internal solution containing 50 μM fura-2 and 6 mM Ca-EGTA plus 3 mM free EGTA. Under our experimental conditions, the mean value of $K_d B$ obtained from five measurements was 1.23 μM. Data analysis was performed and an illustration was made using Clampfit v.6.03 or Origin 3.1.

2.4. Solutions

Modified Krebs solution (mM): 136.6 Na^+, 5.9 K^+, 1.2 Mg^{2+}, 1.2 Ca^{2+}, 47.3 Cl^-, 10 glucose, 10 HEPES: elevated K external solution; 102.5 Na^+, 40 K^+, 1.2 Mg^{2+}, 1.2 Ca^{2+}, 147.3 Cl^-, 10 glucose, 10 HEPES (adjusted at pH 7.4 with Tris base). Low Ca^{2+}-containing and Ca^{2+}-free solutions were made by reducing the concentration of Ca^{2+}; K^+-internal solution for nystatin-perforated recording: 140 K^+, 2 Mg^{2+}, 144 Cl^-, 10 glucose, 10 HEPES (adjusted at pH 7.2 with Tris base); K^+-internal solution for conventional whole-cell recording: 140 K^+, 2.0 Mg^{2+}, 144 Cl^-, 5 phosphocreatine, 5 succinic acid, 1 EGTA, 10 HEPES (adjusted at pH 7.2 with Tris base). Nucleotide phosphates were dissolved to give desired final concentrations just before each experiment (stock solutions were made by dissolving these compounds in solutions of the same composition at 100–400 mM, and stored in a freezer at −20°C); Cs^+ internal solution for conventional whole-cell recording: 140 Cs^+, 2.0 Mg^{2+}, 144 Cl^-, 5 phosphocreatine, 1 Na_2ATP, 10 EGTA, 10 HEPES (adjusted at pH 7.2 with Tris base). Cs^+ internal solution for Ca^{2+} fluorescence measurements: 140 Cs^+, 2 Mg^{2+}, 144 Cl^-, 5 phosphocreatine, 1Na_2ATP, 5 succinic acid, 10 HEPES (adjusted at pH 7.2 with Tris base).

2.5. Chemicals

ATP, ADP, GDP, UDP, ITP, EGTA and fura-2 (pentapotassium salt) were purchased from Dojin (Kumamoto, Japan). Glibenclamide, TEA and 4-aminopyride from Sigma and iberiotoxin and charybtotoxin from Almone. Levcromakalim and MCC-134 were synthesized and kindly provided by Mitsubishi Chemical.

2.6. Statistics

All data are expressed as means ± S.E.M. and two-tailed paired or unpaired *t*-tests, and Tukey's multiple comparison test were employed where appropriate for statistical evaluation.

3. Results

3.1. MCC-134 and levcromakalim activate K^+ currents having similar properties

Fig. 2A shows an actual trace of outward currents appearing upon addition of MCC-134 or levcromakalim in

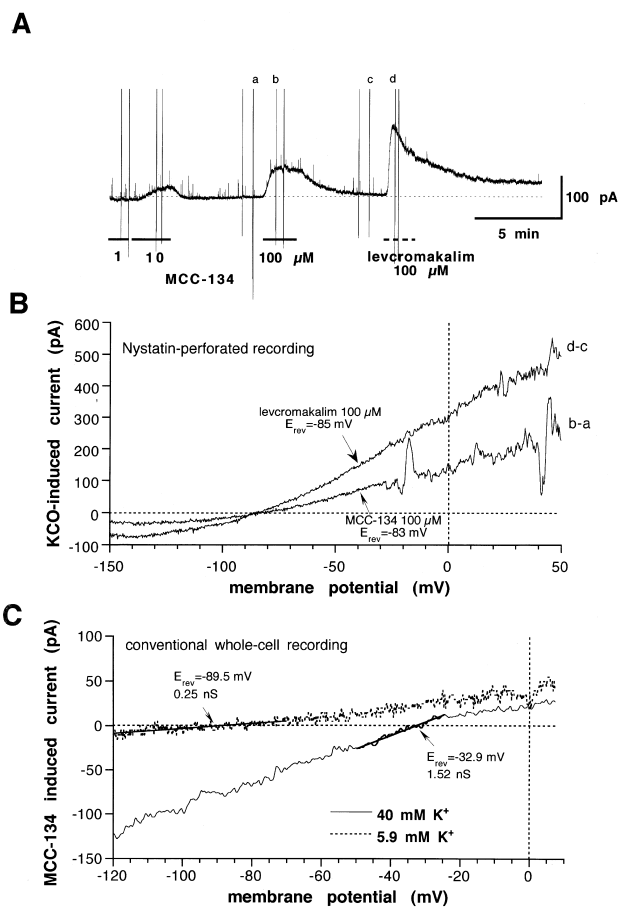

Fig. 2. Outward currents induced by MCC-134 and levcromakalim and their current–voltage ($I-V$) relationships. (A and B) Nystatin-perforated recording with KCl internal solution. The bath contained modified Krebs solution. (A) MCC-134 and levcromakalim were added at the bars. Vertical deflections indicate the currents responding to ramp voltages (−150 to +50 mV, 2 s). Holding potential: −40 mV. Horizontal dotted line represents 0-current level (in this figure and throughout the following figures). (B) $I-V$ relationships of 100 μM MCC-134 (I_{MCC}) and levcromakalim-induced currents (I_{LCRM}). (C) $I-V$ relationships of I_{MCC} with conventional whole-cell recording (K^+ internal solution), with normal (5.9 mM) and elevated (40 mM) K^+ concentrations in the bath. The oblique straight lines indicate the best linear fits of data points.

the bath, recorded at −40 mV with the nystatin-perforated whole-cell clamp technique, under normal ionic conditions. The current components sensitive to MCC-134 (I_{MCC}) or levcromakalim (I_{LCRM}) reversed the polarity close to the estimated K equilibrium potential (E_K) of this muscle (about −80 mV; Fig. 2B). The reversal potential (E_{rev}) of I_{MCC} and I_{LCRM} under these experimental conditions averaged -81 ± 1 ($n = 6$) and -79 ± 1 mV ($n = 9$), respectively, which were not significantly different ($P > 0.05$, with unpaired *t*-test). E_{rev} of I_{MCC} was shifted toward E_K when external K^+ concentration was raised from 5.9 to 40 mM (-33 ± 5 mV, $n = 4$; dotted vs. solid curves in Fig. 2C). This shift is equivalent to 58 mV per tenfold change in external K^+ concentration, suggesting that the current induced by MCC-134 is selective for K^+.

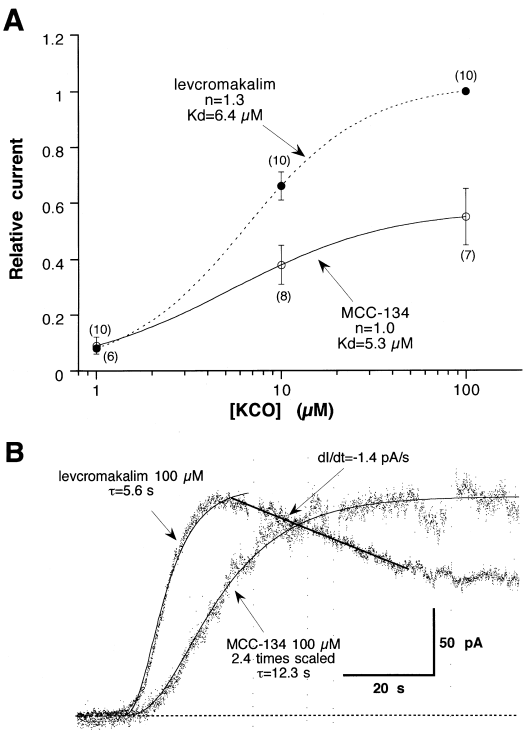

Fig. 3. Concentration–current amplitude relationships and expanded activation time course of I_{MCC} and I_{LCRM}. Recording conditions were the same as in Fig. 2A. (A) Relationships between the concentration of MCC-134 or levcromakalim and the amplitude of outward current. Smooth curves are the results of Hill fitting of data points; $I = I_{max}/(1 + (K_d/[Drug])^n$, where I, I_{max}, K_d, [Drug] and n denote the current amplitude at a given concentration, its maximum, apparent dissociation constant, drug concentration, and cooperativity coefficient, respectively. To minimize the variation arising from different cells, the current amplitude is normalized to that for 100 μM levcromakalim. (B) Activation and desensitization time courses of scaled I_{MCC} and I_{LCRM}. Traces (dots) are expanded for the first 100 s from the parts corresponding to application of 100 μM MCC-134 and levcromakalim in Fig. 2A. Solid curves are drawn according to the results of the best fit with a power exponential function: $I = I_{max}(1 - \exp(-t/\tau))^{3.5}$, where I_{max}, t and τ denote the peak amplitude, time from the onset of drug application and time constant of activation, respectively. Thick straight line represents the best linear fit of data points for the declining phase of I_{LCRM}. For better comparison, the peak amplitude of I_{MCC} is scaled up 2.4 times to match that of I_{LCRM}.

The current–voltage relationship of I_{MCC} evaluated with elevated external K^+ concentration (40 mM) shows no obvious deviation from the linearity in its inward portion, indicating virtual lack of voltage dependence, although in the outward portion a slight flattening, presumably due to internal Mg^{2+} blockade (solid curve in Fig. 2C).

The magnitude and activation of I_{MCC} became larger and faster, respectively (Fig. 2), as the concentration of MCC-134 was raised higher; this finding was also true for levcromakalim (not shown). As summarized in Fig. 3A, the concentration–current amplitude relationship gives similar EC_{50} values for MCC-134 and levcromakalim (5.3 and 6.4 μM, respectively), suggesting both K^+ channel openers have similar affinity as ligands. In contrast, MCC-134 was always found less effective to activate the outward current than levcromakalim (see Fig. 2A). The maximum response induced by MCC-134 was on average only about a half of that by levcromakalim (Fig. 3A). The time course of activation was also found slower for I_{MCC} than I_{LCRM} when compared in the same cell. Fitting the rising phase of their activation by a power exponential function gives about a twice longer time constant for I_{MCC} than I_{LCRM} (12.3 vs. 5.6 s; Fig. 3B). This observation was consistently obtained in almost all tested cells; the time required for 10%–50% activation was 19.5 ± 6.5 s and 6.8 ± 0.8 s for I_{MCC} and I_{LCRM} respectively ($n = 10$; $P < 0.05$ with paired *t*-test). In addition to these, two other important differences were noted between I_{MCC} and I_{LCRM}. Firstly, even in the continued presence of drug, the amplitude of I_{MCC} stayed almost constant, whereas that of I_{LCRM} was decreased rapidly (straight line in Fig. 3B; see also Fig. 2A). At the maximally effective concentration of 100 μM, the rate of this desensitization (measured for the first 10 s from the peak response) was as small as 3.6 ± 1.5% of the peak for I_{MCC}, while it amounted to 14.5 ± 2.0% for I_{LCRM} ($n = 10$; $P < 0.001$ with paired *t*-test). Secondly, the time course of deactivation that occurs upon drug washout was obviously much faster for I_{MCC} than I_{LCRM}. The time required for 100–50% deactivation was 32 ± 7 s and 140 ± 18 s for I_{MCC} and I_{LCRM}, respectively ($n = 10$; $P < 0.001$ with paired *t*-test); at a concentration of 100 μM, I_{LCRM} persisted over 10 min despite continuous washout of the drug. Taken together, these results suggest strongly that, although both K^+ channel openers would target the same type of K^+ channels, the actions of MCC-134 may be slower in onset, weaker in efficacy, long-lasting (owing to less marked desensitization) and more readily reversible than levcromakalim.

The amplitude of I_{MCC} with 5.9 mM external K^+ was small especially when recorded by conventional, instead of nystatin-perforated, whole-cell recording. This often hampered a quantitative evaluation of the effects of drugs and compounds tested on a statistical basis. Thus, in the rest of this study, I_{MCC} was recorded mostly as an inward current, by elevating the external K^+ concentration to 40 mM. This procedure is expected to relieve the blocking action of

intracellular Mg^{2+} (Nelson and Quayle, 1995) as well as to increase the slope conductance of the current (see the solid vs. dotted curves in Fig. 2C).

3.2. Pharmacological similarities between I_{MCC} and I_{LCRM}

As demonstrated in Fig. 4Aa, I_{MCC} was, even near-maximally activated, completely inhibited by addition of 10 μM glibenclamide, the specific blocker of ATP-sensitive K^+ channels. In contrast, specific blockers of several distinct types of Ca^{2+}-dependent K^+ channels, iberiotoxin (500 nM), charybdotoxin (200 nM; Fig. 4Ab) and apamin (500 nM) were all ineffective at suppressing I_{MCC} (Fig. 4B). On the other hand, nonspecific K^+ channel blockers such as tetraethylammonium, 4-aminopyridine, and Ba^{2+} differentially inhibited the currents (Fig. 4Ac and d). Fig. 4B summarizes this series of experiments. The IC_{50} values of glibenclamide, 4-AP and Ba^{2+} were in the range of 0.1–1 μM, 1–10 mM, 0.1–1 mM and 0.01–0.1 mM, respectively. Similar extents of inhibition were also observed for I_{LCRM} with glibenclamide (10 μM; 2 ± 1% of control; $n = 4$), tetraethylammonium (1 and 10 mM; 83 ± 5 and 35 ± 4% of control, $n = 3$, respectively), and Ba^{2+} (1 mM; 17 ± 6% of control, $n = 7$). The observed pharmacological profile of I_{MCC} with I_{LCRM}, most likely consistent with that of glibenclamide-sensitive K^+ channels so far reported in smooth muscle (Nelson and Quayle, 1995).

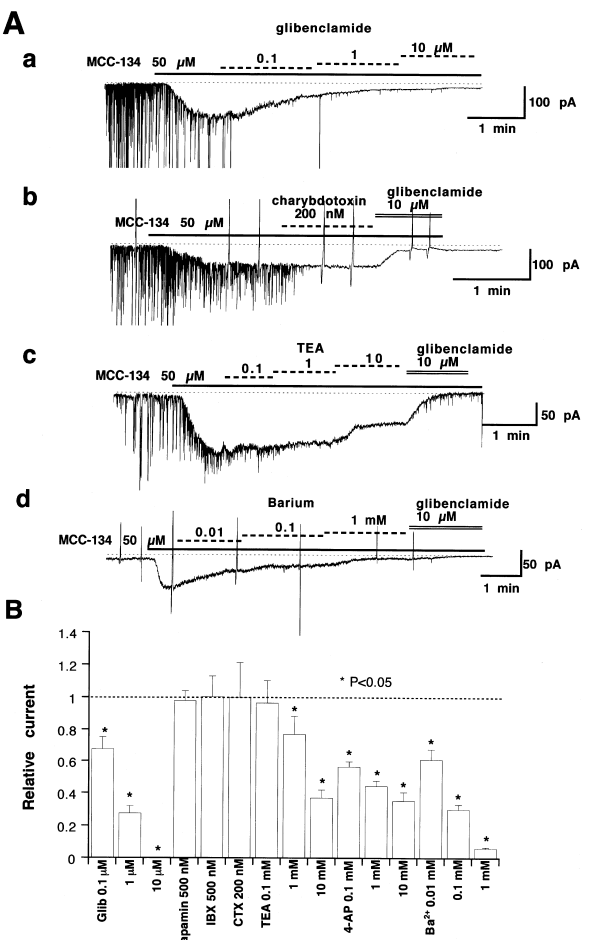

Fig. 4. Pharmacological profile of I_{MCC}. Recording conditions were the same as in Fig. 2C. (A) Timing of drug application is indicated by bars. Holding potential: −40 mV. Irregular intermittent inward deflections represent spontaneous transient K^+ currents, which reflect the cyclical release of Ca^{2+} from the internal store (see Bolton and Imaizumi, 1996). Sharp vertical outward deflections indicate ramp voltage-induced currents. (B) Summary of experiments as shown in A ($n = 3$–7). Asterisks indicate statistically significant differences with paired *t*-test. Abbreviations: Glib., glibenclamide: IBX, iberiotoxin: CTX, charybdotoxin; TEA, tetraethylammonium.

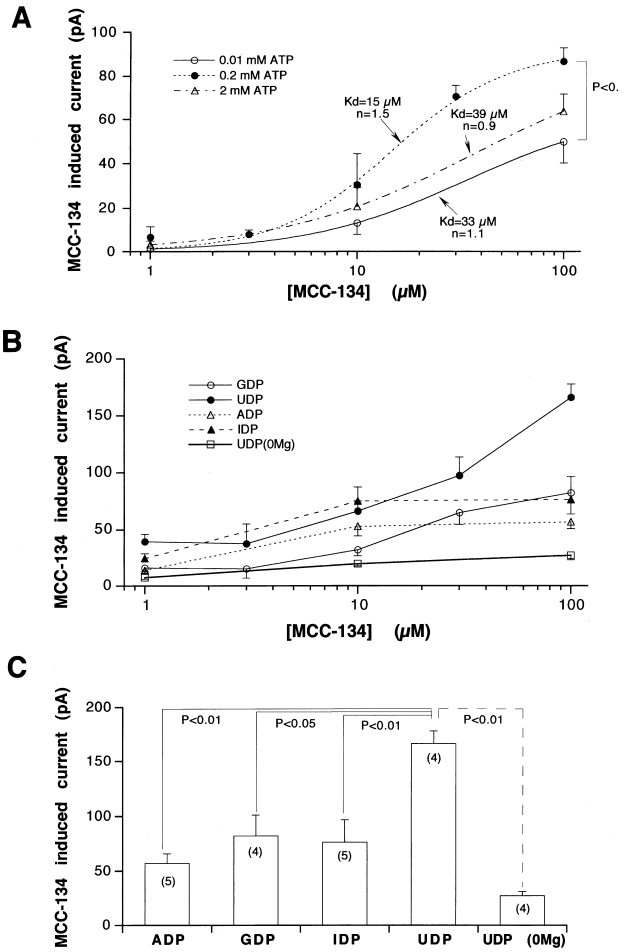

Fig. 5. Effects of nucleotide phosphates on I_{MCC}. Experimental conditions were the same as in Fig. 2C (with elevated external K^+). (A) Concentration–current amplitude relationships for I_{MCC} with 0.01, 0.2 and 2 mM ATP in the pipette. Smooth curves indicate the best fit of Hill fitting of data points (the results labeled in the figure). The value ($P < 0.01$) on the right means a statistically significant difference between filled (0.2 mM ATP) and open circles (0.01 mM ATP) at 100 μM MCC-134, with Tukey's test. The number of experiments is 4–15 for each data point. (B) Concentration–current amplitude relationships for I_{MCC} with 2 mM Mg^{2+} plus 1 mM GDP, UDP, or ADP, and 1 mM UDP alone in the pipette. The number of experiments is 3–7 for each data point. (C) Efficacy of nucleotide diphosphate (1 mM) at activating I_{MCC} (100 μM). *P* values with solid line are the results of Tukey's test, while that with dotted line (right) with unpaired *t*-test.

3.3. Nucleotide phosphate dependence

When the concentration of ATP in the pipette was varied 0.01, 0.2 and 2 mM, the concentration–current amplitude relationship for I_{MCC} showed a biphasic dependence on ATP concentration (Fig. 5A). Apparent EC_{50} values and maximum responses estimated from empirical Hill analysis indicated that the affinity and efficacy of MCC-134 would be greatest at 0.2 mM (dotted curve in Fig. 5A), while they decreased at lower and higher concentrations of ATP. These findings are similar to those obtained in various types of smooth muscle cells (Bonev and Nelson, 1993; Kleppisch and Nelson, 1995; Wellman et al., 1998). In another set of experiments, we tested the effects of intracellular nucleotide diphosphates (1 mM) such as ADP, GDP, IDP and UDP on I_{MCC} without including ATP in the pipette. As summarized in Fig. 5B, even in the sole presence of nucleotide diphosphates,

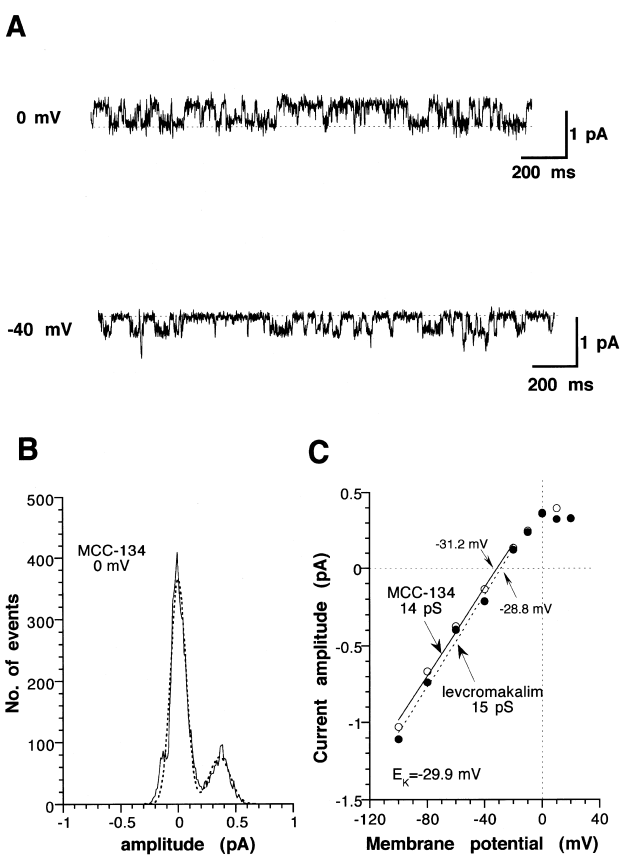

Fig. 6. Single K^+ channel activities induced by MCC-134. The cell-attached mode. 100 μM MCC-134 was present in the patch pipette. In order to eliminate the transmembrane K^+ gradient, external K^+ concentration was raised to 140 mM. Thus, the transmembrane potential of patch membrane can be defined as the inverse of the pipette potential. (A) Actual traces of single channel activities in the presence of MCC-134 (100 μM), at two different membrane potentials. (B) Amplitude histogram constructed for the channel activities at 0 mV (solid curve). Dotted curve indicates the results of Gaussian fit with two peaks. (C) $I-V$ relationships for MCC-134 (open circles) and levcromakalim (closed circles) induced single channel currents and their linear regression (solid and dashed lines, respectively).

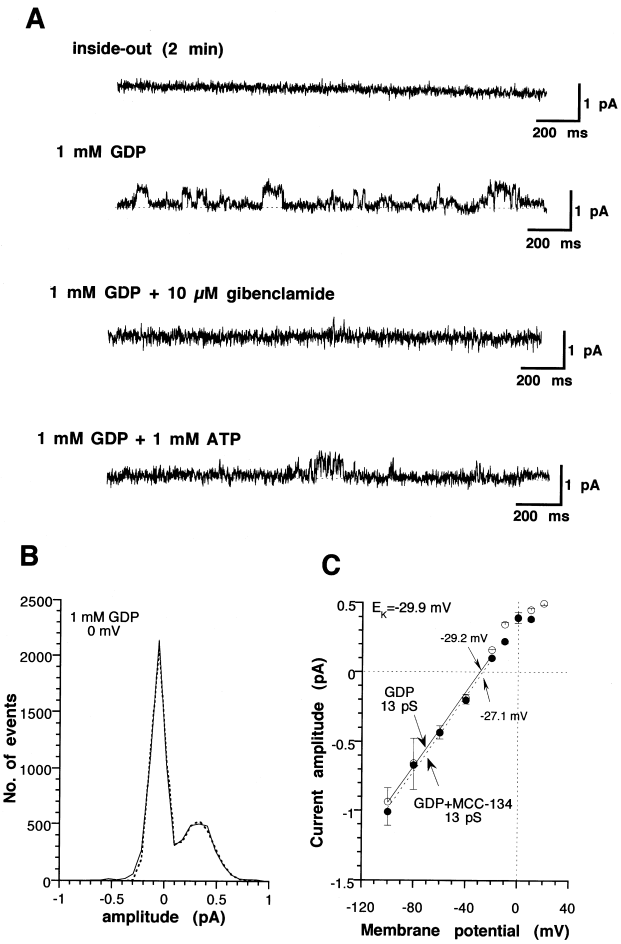

Fig. 7. Properties of GDP-induced single channel activities. The inside-out mode at 0 mV. Bath contained 140 mM KCl solution. (A) Single channel activities completely disappeared approximately 2 min after patch excision into the bath solution (top trace). Addition of 1 mM GDP (with 2 mM Mg^{2+}) into the bath induced outward fluctuating single channel activities (second trace), which were strongly inhibited by 10 μM glibenclamide (third trace) or 1 mM ATP (bottom trace). (B) Amplitude histogram at 0 mV in the presence of 1 mM GDP in the bath. (C) $I-V$ relationships of GDP-induced channel currents and their linear regression in the absence (open circles and solid line) and presence (closed circles and dashed line) of 100 μM MCC-134 in the pipette.

MCC-134 was still able to activate the current dose-dependently, which, however seemed to need the presence of Mg^{2+}, since vigorous chelation of Mg^{2+} with 2 mM EDTA almost completely abolished the effects of MCC-134 (open squares in Fig. 5B). At the maximally effective concentration of MCC-134, 100 μM, the apparent efficacy sequence of nucleotide diphosphate for activating I_{MCC} was UDP > IDP≒DP ≧ ADP (Fig. 5C). We also tested the effects of MCC-134 in the combined presence of ATP and UDP (1 mM) in the pipette, the results supporting the biphasic action of ATP on I_{MCC} (data not shown).

3.4. Single channel recording

Fig. 6A displays single channel activities recorded at two different pipette potentials (0 and 40 mV; thus the

estimated membrane potential is 0 and −40 mV, respectively) in the cell-attached mode (for detail see the legend to Fig. 6A). The current–voltage (I–V relationship constructed from the unitary amplitude of these channel activities shows a slight inward rectification. The linear (inward) portion of the I–V curve gives a conductance of ca. 15 pS and a reversal potential of ca. −30 mV, which is close to the calculated E_K (open circles and solid line in Fig. 6C; see the legend to Fig. 6C). The curve is almost superimposable on that constructed from levcromakalim-activated single channel activities under the same experimental conditions (solid circles and dotted curve in Fig. 6C).

MCC-134-induced channel activities, which were usually sustained over 10 min in the cell-attached mode, were abolished by addition of 10 μM glibenclamide in the bath, and disappeared upon excision of the patch membrane (i.e., inside-out mode; top trace in Fig. 7A). However, similar channel activities, having an almost identical amplitude, were restored by subsequent application of 1 mM GDP and Mg^{2+} to the cytosolic face of patch membrane, regardless of the presence of MCC-134 in the pipette (the second trace in Fig. 7A). The GDP-induced channel activities did not differ essentially from those induced by MCC-134 observed in cell-attached mode, in unitary conductance and reversal potential (Fig. 7C), and were strongly inhibited by 1 mM ATP or 10 μM glibenclamide (the third and bottom traces in Fig. 7A). Qualitatively similar observations were obtained with ADP, ITP or UTP instead of GDP (data not shown).

We also tested the effects of intracellular ATP alone in the inside-out patch mode. Although no channel openings were detected in the sole presence of ATP (0.01, 0.1, 1 and

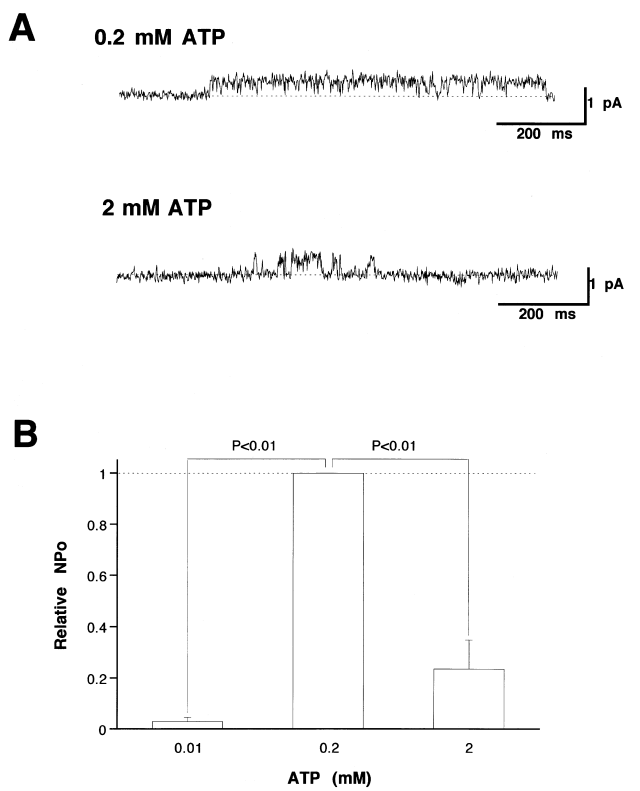

Fig. 8. ATP dependence of MCC-134-induced single channel activities. The same recording conditions as in Fig. 7. (A) Representative records of MCC-134 (100 μM)-induced K^+ channel activities in the presence of 0.2 (top trace) or 2 mM (second trace) ATP at the cytoplasmic side of patch membrane. (B) Summary of experiments as shown in panel A. NP_o is defined as $(\Sigma t_i)/T$, where t_i and T denote the duration of ith opening induced by MCC-134 and total recording time (10 min), respectively. In the figure, NP_o is further normalized to that with 0.2 mM ATP, which was taken as a control in each experiment. P values indicate the results of paired t-test.

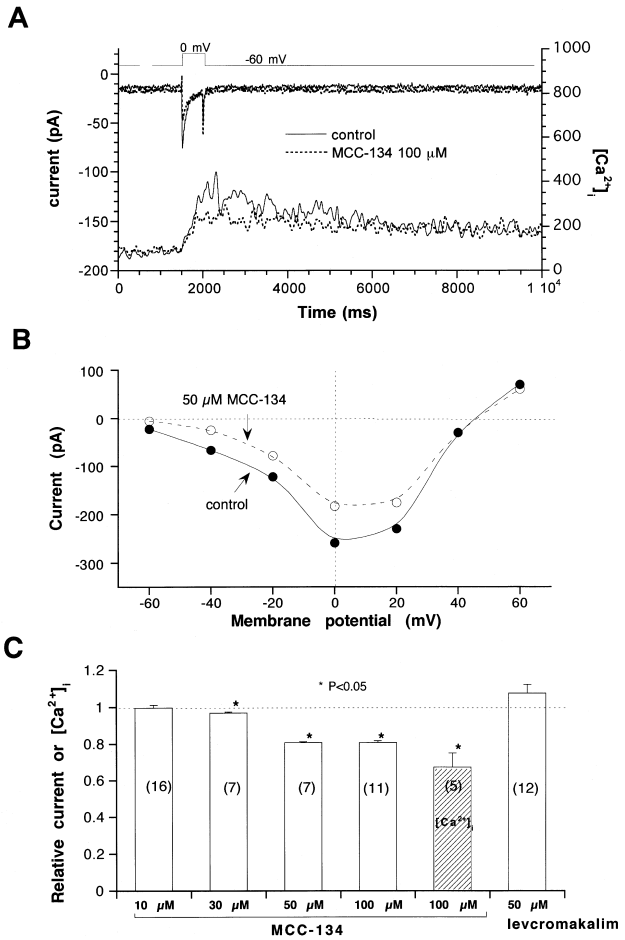

Fig. 9. MCC-134 inhibits voltage-dependent Ca^{2+} currents. Bath and pipette contained modified Krebs and Cs^+-internal solutions, respectively. (A) Simultaneous recording of Ca^{2+} currents (upper traces) and concomitant rises in $[Ca^{2+}]_i$ (lower traces) evoked in response to a depolarizing pulse to mV, in the absence (solid curves) and presence (dotted curves) of 100 μM MCC-134, in a 50-μM fura-2-loaded cell. (B) I–V relationship of voltage-dependent Ca^{2+} current in the absence (closed circles) and presence (open circles) of 50 μM MCC-134 in the bath. The curves were obtained with 200-ms depolarizing pluses from a holding potential of −80 mV with an interval of 30 s. (C) Summary of inhibition by MCC-134 of Ca^{2+} current (0 mV; open columns) and $[Ca^{2+}]_i$ rise (hatched column). For better comparison, the effect of 50-μM levcromakalim on Ca^{2+} current is also shown on the rightmost part. Asterisks indicate statistically significant differences with paired t-test.

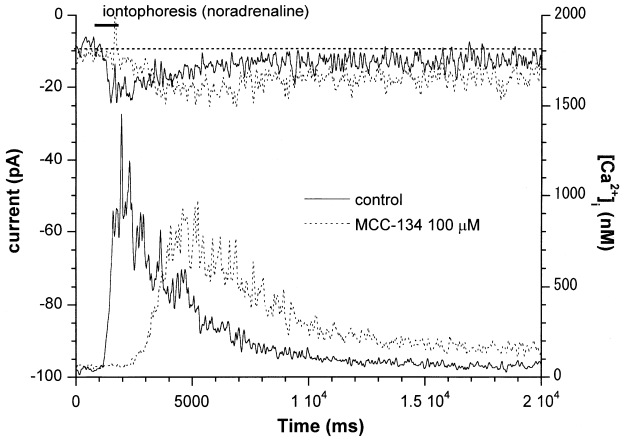

Fig. 10. MCC-134 inhibits noradrenaline-induced Ca^{2+} mobilization and cation current simultaneous recording of cation currents (upper traces) and concomitant rises in $[Ca^{2+}]_i$ (lower traces) evoked by iontophoretically applied noradrenaline (0.1 M, 50 nA, 1 s; a maximally effective dose), in the absence (solid curves) and presence (dotted curves) of 100 μM MCC-134, in a 50 μM fura-2 loaded cell.

3 mM; $n = 3$, respectively; data not shown), a biphasic dependence on cytoplasmic ATP concentration (0.01,0.2, 2 mM), which was observed for I_{MCC} (Fig. 5A), was also observed on single channel activities induced by MCC-134 (Fig. 8).

3.5. MCC-134 affects $[Ca^{2+}]_i$ elevations evoked by depolarization and noradrenaline

MCC-134, in addition to its K^+ channel activating ability, exerted nonspecific actions on two major Ca^{2+}-mobilizing mechanisms in this muscle. As shown in Fig. 9, both Ca^{2+} currents and concomitant rises in $[Ca^{2+}]_i$ evoked by depolarizing pulses, were significantly inhibited by 20–30% by MCC-134 at higher concentrations than required to open K^+ channels (50–100 μM; Fig. 9C). In contrast, levcromakalim was found ineffective at inhibiting the current, up to 50 μM (Fig. 9C).

MCC-134 also affected the time course of $[Ca^{2+}]_i$ elevation and accompanying inward cationic current induced by noradrenaline (Fig. 10). Although the peak response was not clearly inhibited, a considerable lag to the peak was observed in both the $[Ca^{2+}]_i$ rise and cation current (dotted curves in Fig. 10). Similar results were obtained in two other cells.

4. Discussion

The main results of the present study are that MCC-134 activates ATP-sensitive, GDP activatable K^+ channels, the properties of which are very similar to those so far described in various types of smooth muscle cells. The unitary conductance of 13–15 pS with 40/140 mM extra-/intracellular K^+ is comparable to those of small conductance, glibenclamide-sensitive, nucleotide diphosphate-activatable K^+ channels reported for the same preparation (15 pS with 6/140 mM K^+, Kajioka et al., 1991; 24 pS with 60/130 mM K^-, Beech et al., 1993) and other vascular smooth muscles (so-called K_{NDP}; rat mesenteric artery, 20 pS with 60/130 mM, Zhang and Bolton, 1995). Rapid rundown upon patch membrane excision, direct restoration of channel activities by submillimolar GDP (Mg^{2+} required) and subsequent inhibition by millimolar concentrations of ATP are also commonly observed features in this type of channel (Kajioka et al., 1991; Beech et al., 1993; Kamouchi and Kitamura, 1994; for review, Quayle et al., 1997). Many of these features were confirmed at the whole-cell current level as well. Furthermore, levcromakalim, an established potent K^+ channel opener (Edwards and Weston, 1993) also activated whole-cell currents having similar pharmacological properties and single channel currents with an almost identical conductance to MCC-134-induced currents. These results strongly support the view that K^+ channels activated by MCC-134 belong to the same class of K^+ channels as the small conductance, glibenclamide-sensitive K^+ channels or K_{NDP}.

K^+ channel openers target several distinct classes of K^+ channels. For example, in canine colonic smooth muscle cells, the activity of large conductance Ca^{2+}-activated K^+ channels (K_{Ca}) were enhanced by cromakalim, which was then antagonized by glibenclamide (Carl et al., 1992). In our experiments, contribution of K_{Ca} could be largely excluded, since specific blockers of K_{Ca}, charybdotoxin and iberiotoxin, were found to be ineffective at inhibiting the whole-cell I_{MCC}. Furthermore, the observed sensitivities of I_{MCC} to tetraetylammonium, 4-aminopyridine and Ba^{2+} are not compatible with those of delayed or inward rectifying K^+ currents, although the hypothesis of 'conversion' of delayed rectifier K^+ channels to the K_{ATP} by levcromakalim has recently been proposed (Edwards et al., 1993). These results largely exclude the contribution of these channels to the genesis of I_{MCC} (Nelson and Quayle, 1995; Quayle et al., 1997). In cardiac and pancreatic β-islet cells, large conductance, highly ATP-sensitive K^+ channels have been reported to be activated by K^+ channel openers. Although K^+ channels of similar properties have also been found in a certain type of vascular smooth muscle (rat portal vein, LK channels; Zhang and Bolton, 1996), we could not see the counterpart of LK channels in the rabbit portal vein, which should be transiently activated by membrane excision in the absence of K^+ channel opener. These results suggest that MCC-134 is relatively selective for activating the small conductance glibenclamide-sensitive K^+ channels.

Recent molecular cloning studies have suggested that combination of two inward-rectifier K^+ channels (Kir6.1 or 6.2) with three distinct sulfonylurea receptors (SUR1, 2A or 2B) can reconstitute the major biophysical and pharmacological properties of native ATP-sensitive K^+

channels, such as differential sensitivities to glibenclamide, K^+ channel openers, intracellular ATP or nucleotide diphosphates (Quayle et al., 1997; Yamada et al., 1997; Aguilar-Brayan et al., 1998). Among them, the combination of Kir 6.1 and SUR2B most closely mimics K_{NDP} (Yamada et al., 1997). The mechanism for activating this recombinant channel by K^+ channel openers is essentially different from that for cardiac ATP-sensitive K^+ channels, where the main effect of K^+ channel openers is to shift the ATP concentration–channel activity (inhibition) curve toward higher concentrations (Terzic et al., 1995). In the Kir6.1/SUR2B complex channel, nucleotide triphosphates and diphosphates such as ATP, GTP, ADP and GDP exhibit both activating and inhibitory effects, thus rendering the nucleotide triphosphates (nucleotide diphosphate) concentration-channel activity curve bell-shaped in the range of 0.1 μM–10 mM. K^+ channel openers raise the peak of this curve and shift it toward lower concentrations, by potentiating the activating effect of nucleotide triphosphates (nucleotide diphosphate) (Satoh et al., 1998). The inhibitory effect of nucleotide triphosphates (nucleotide diphosphate) is not evident with UTP or UDP at a concentration up to 10 mM. Thus, the apparent efficacy of K^+ channel openers becomes most prominent with UTP or UDP in this concentration range (Satoh et al., 1998). These properties are apparently consistent with our present observations; the intracellular ATP had a biphasic effect on both I_{MCC} and single channel activities induced by MCC-134, with an apparent peak at 0.2 mM (Figs. 5A and 8; compare with Fig. 2 in Satoh et al., 1998). UDP, at a concentration of 1 mM, exhibited a greater efficacy to activate I_{MCC} than other nucleotide diphosphates (Fig. 5C; see also Kamouchi and Kitamura, 1994). Obviously, more information about the effects of nucleotide triphosphates (nucleotide diphosphates) over a broader concentration range with and without K^+ channel openers will be required to determine whether the nucleotide triphosphate (or nucleotide diphosphate) dependence of the Kir6.1/SUR2B complex channel can fully account for that of native K_{NDP} such as in our preparation.

Our other lines of evidence have suggested that MCC-134 nonspecifically suppresses Ca^{2+} mobilization through both voltage-dependent and receptor-operated routes, at near maximally effective concentrations. Similar observations have been reported with several K^+ channel openers having different structures. For example, in rabbit mesenteric artery, pinacidil has been found to reduce noradrenaline-induced IP_3 production and thereby attenuate a subsequent Ca^{2+} transient and tension development (Itoh et al., 1992). Although this has been attributed to the membrane hyperpolarization induced by pinacidil per se and a later patch clamp study has confirmed this possibility (Ganitkevich and Isenberg, 1993), our results have shown that even under the voltage-clamped conditions MCC-134 retarded the development of both noradrenaline-induced Ca^{2+} transients and concomitant inward cation currents (Fig. 10). The discrepancy could partly be accounted for by the other actions of K^+ channel openers, e.g., inhibition of Ca^{2+} re-uptake into the internal store (Aaronson and Benham, 1996), but we did not pursue this speculation in further detail. The inhibitory effect of MCC-134 on the voltage-dependent Ca^{2+} currents may be peculiar to this drug, since almost all K^+ channel openers have been shown not to affect this current (but see Okabe et al., 1990). Indeed, no such effect was observed for levcromakalim in our study (Fig. 9). Although the detailed mechanism remains unclear, it is conceivable that the mild inhibitory effect of MCC-134 on the voltage-dependent Ca^{2+} channel may act synergistically with its K^+-channel activating action to relax the vascular smooth muscle more effectively.

In summary, MCC-134, like levcromakalim, can induce the outward current having a comparable magnitude to other K^+ channel openers under the quasi-physiological conditions (Fig. 2). The channels responsible for this current seem to have almost the same properties as described previously (K_{NDP}) in many biophysical and pharmacological respects. From a clinical point of view, however, this drug may have a number of advantages over other K^+ channel openers; its extremely slow-desensitizing and fast deactivating properties might help the drug to work in a long-lasting manner, and make it easy control its effective concentration in the blood. Furthermore, nonspecific but moderate inhibitory actions on two major Ca^{2+} mobilizing mechanisms may further reinforce the vasorelaxant effect of this drug as a K^+ channel opener. In addition, MCC-134 has been reported to decrease the Ca^{2+}-sensitivity of the contractile machinery in aortic smooth muscle (Seino et al., 1996; see also Itoh et al., 1991) and lower the plasma triglyceride level in Zucker fatty rats, which is often found to be elevated in the patients of essential hypertension who have atherosclerotic changes (Umeda et al., 1997b). These features might altogether work toward normalizing the elevated blood pressure and presumably ameliorating other associated disorders.

References

Aaronson, P.I., Benham, C.D., 1996. Potassium channel electrophysiology in vascular smooth muscle cells and the site of action of potassium channel openers. In: Evans, J.M., Hamilton, T.C., Longman, S.D., Stemp, G. (Eds.), Potassium Channels and their Modulators: From Synthesis to Clinical Experience. Taylor & Francis, London, pp. 157–172.

Aguilar-Bryan, L., Clement, J.P. IV, Gonzalez, G., Kunjilwar, K., Babenko, A., Bryan, J., 1998. Toward understanding the assembly and structure of K_{ATP} channels. Physiol. Rev. 78, 227–245.

Almers, W., Neher, E., 1985. The Ca signal from fura-2 loaded mast cells depends strongly on the method of dye-loading. FEBS Lett. 192, 13–18.

Beech, D.J., Zhang, H., Nakao, T., Bolton, T.B., 1993. Single channel and whole-cell K currents evoked by levcromakalim in smooth muscle cells from the rabbit portal vein. Br. J. Pharmacol. 110, 538–590.

Bolton, T.B., Imaizumi, Y., 1996. Spontaneous transient outward currents in smooth muscle cells. Cell Calcium 20, 141–152.

Bonev, A.D., Nelson, M.T., 1993. ATP-sensitive potassium channels in smooth muscle cells from guinea-pig urinary bladder. Am. J. Physiol. 264, C1190–C1200.

Carl, A., Brown, S.M., Gelband, K.M., Sanders, K.M., Hume, J.R., 1992. Cromakalim and lemakalim activates Ca^{2+} dependent K^+ channels in canine colon. Pflügers Arch. 421, 67–76.

Edwards, G., Weston, A.H., 1993. The pharmacology of ATP-sensitive potassium channels. Annu. Rev. Pharmacol. Toxicol. 33, 597–637.

Edwards, G., Ibbotson, T., Weston, A.H., 1993. Levcromakalim may induce a voltage-independent K^+-current in rat portal veins by modifying the gating properties of the delayed rectifier. Br. J. Pharmacol. 110, 1037–1048.

Evans, J.M., Hamilton, T.C., Longman, S.D., Stemp, G., 1996. Potassium Channels and their Modulators: From Synthesis to Clinical Experience. Taylor & Francis, London.

Ganitkevich, V.Y., Isenberg, G., 1993. Membrane potential modulates inositol 1,4,5-trisphosphate-mediated Ca^{2+} transients in guinea-pig coronary myocytes. J. Physiol. 470, 35–44.

Grynkiewicz, G., Poenie, M., Tsien, R.Y., 1985. A new generation of Ca^{2+} indicators with greatly improved fluorescence properties. J. Biol. Chem. 260, 3440–3450.

Inoue, R., Kuriyama, H., 1993. Dual regulation of cation-selective channels by muscarinic and α_1-adrenergic receptors in the rabbit portal vein. J. Physiol. 465, 427–448.

Itoh, T., Suzuki, S., Kuriyama, H., 1991. Effects of pinacidil on contractile proteins in high K^+-treated intact, and β-escin-treated skinned smooth muscle of the rabbit mesenteric artery. Br. J. Pharmacol. 103, 1697–1702.

Itoh, T., Seki, N., Suzuki, S., Ito, S., Kajikuri, J., Kuriyama, H., 1992. Membrane hyperpolarization inhibits agonist-induced synthesis of inositol 1,4,5-trisphosphate in rabbit mesenteric artery. J. Physiol. 451, 307–328.

Kajioka, S., Kitamura, K., Kuriyama, H., 1991. Guanosine phosphate activates an adenosine 5′-trisphosphate-sensitive K^+ channel in the rabbit portal vein. J. Physiol. 444, 397–418.

Kamouchi, M., Kitamura, K., 1994. Regulation of ATP-sensitive and nucleotide diphosphate in rabbit portal vein. Am. J. Physiol. 266, H1687–H1698.

Kleppisch, T., Nelson, M.T., 1995. ATP-sensitive K^+ currents in cerebral arterial smooth muscle: pharmacological and hormonal modulation. Am. J. Physiol. 269, H1634–H1640.

Morita, H., Inoue, R., Ito, Y., 1998. ABA-267, a novel potassium channel opener, activates K_{NDP}-like channels in rabbit portal vein. Jpn. J. Pharmacol. 76, 76P.

Nelson, M.T., Quayle, J.M., 1995. Physiological roles and properties of potassium channels in arterial smooth muscle. Am. J. Physiol. 268, C799–C822.

Nelson, M.T., Patlak, J.B., Worley, J.F., Standen, N.B., 1990. Calcium channels, potassium channels and voltage dependence of arterial smooth muscle tone. Am. J. Physiol. 259, C3–C18.

Okabe, K., Kajioka, S., Nakao, K., Kitamura, K., Kuriyama, H., Weston, A.H., 1990. Actions of cromakalim on ionic currents recorded from single smooth muscle cells of the rat portal vein. J. Pharmacol. Exp. Ther. 250, 832–839.

Quayle, J.M., Nelson, M.T., Standen, N.B., 1997. ATP-sensitive and inwardly rectifying potassium channels in smooth muscle. Physiol. Rev. 77, 1165–1232.

Satoh, E., Yamada, M., Kondo, C., Repunte, V.P., Horio, Y., Iiijima, T., Kurachi, Y., 1998. Intracellular nucleotide-mediated gating of SUR/Kir6.0 complex potassium channels expressed in a mammalian cell line and its modification by pinacidil. J. Physiol. 511, 663–674.

Seino, A., Bessho, H., Ishibashi, A., Nagano, T., Shinpuku, T., Tutsui, M., Okushima, H., Narimatsu, A., 1996. Characterization of vasorelaxant action of MCC-134, a novel benzopropanethioamide derivative. Jpn. J. Pharmacol. 71, 141P.

Shinpuku, T., Tsutsui, M., Nagano, T., Sekiya, T., Okushima, H., Bessho, H., Umeda, A., Narimatsu, A., 1997. Chem. Pharm. Bull. 26, 1P.

Terzic, A., Jahangir, A., Kurachi, Y., 1995. Cardiac ATP-sensitive K^+ channels: regulation by intracellular nucleotides and K^+ channel-opening drugs. Am. J. Physiol. 269, C525–C545.

Umeda, A., Bessho, H., Abe, Y., Ohishi, H., Kitada, Y., 1997a. Antihypertensive and cardiohemodynamic effects of a novel vasodilator MCC-134 in rats and dogs. Jpn. J. Pharmacol. 73, 133P.

Umeda, A., Bessho, H., Abe, Y., Kitada, Y., 1997b. Effect of MCC-134, a novel antihypertensive agent, on lipid metabolism and vascular smooth muscle cell proliferation in rats. Atherosclerosis 134, 135P.

Wellman, G.C., Quayle, J.M., Standen, N.B., 1998. ATP-sensitive K^+ channel activation by calcitonin-gene-related peptide and protein kinase A in pig coronary arterial smooth muscle. J. Physiol. 507, 117–129.

Yamada, M., Isomoto, S., Matsumoto, S., Kondo, C., Shindo, T., Horio, Y., Kurachi, Y., 1997. Sulphonylurea receptor 2B and Kir6.1 form a sulphonylurea-sensitive but ATP-sensitive K^+ channel. J. Physiol. 499, 715–720.

Zhang, H.-L., Bolton, T.B., 1995. Activation by intracellular GDP, metabolic inhibition and pinacidil of a glibenclamide-sensitive K^+ channel in smooth muscle cells of rat mesenteric artery. Br. J. Pharmacol. 114, 662–672.

Zhang, H.-L., Bolton, T.B., 1996. ATP-sensitive potassium channels and their modulation by nucleotides and potassium channel openers in vascular smooth muscle cells. In: Bolton, T.B., Tomita, T. (Eds.), Smooth Muscle Excitation. Academic Press, London, pp. 75–82.